HHS Public Access

Author manuscript

Schizophr Res. Author manuscript; available in PMC 2019 January 03.

Published in final edited form as:

Schizophr Res. 2018 November ; 201: 208–216. doi:10.1016/j.schres.2018.04.029.

Resting-state network connectivity and metastability predict clinical symptoms in schizophrenia

Won Hee Lee, **Gaelle E. Doucet**, **Evan Leibu**, and **Sophia Frangou***

Department of Psychiatry, Icahn School of Medicine at Mount Sinai, New York, NY 10029, USA

Abstract

Background: The functional architecture of resting-state networks (RSNs) is defined by their connectivity and metastability. Disrupted RSN connectivity has been amply demonstrated in schizophrenia while the role of metastability remains poorly defined. Here, we undertake a comprehensive characterisation of RSN organization in schizophrenia and test its contribution to the clinical profile of this disorder.

Methods: We extracted RSNs representing the default mode (DMN), central executive (CEN), salience (SAL), language (LAN), sensorimotor (SMN), auditory (AN) and visual (VN) networks from resting-state functional magnetic resonance imaging data obtained from patients with schizophrenia ($n = 85$) and healthy individuals ($n = 48$). For each network, we computed its functional cohesiveness and integration and used the Kuramoto order parameter to compute metastability. We used stepwise multiple regression analyses to test these RSN features as predictors of symptom severity in patients.

Results: RSN features respectively explained 14%, 17%, 12% and 5% of the variance in positive, negative, anxious/ depressive and agitation/disorganization symptoms. Lower functional integration between the DMN, CEN and SMN primarily contributed to positive symptoms. The functional properties of the SAL network were key predictors of all other symptom dimensions; specifically, lower cohesiveness of the SAL, lower integration of this network with the LAN and higher integration with the CEN respectively contributed to negative, anxious/depressive and disorganization symptoms. Increased SAL metastability was associated with negative symptoms.

Conclusions: These results confirm the primacy of the SAL network for schizophrenia and demonstrate that abnormalities in RSN connectivity and metastability are significant predictors of schizophrenia-related psychopathology.

*Corresponding author at: Department of Psychiatry, Icahn School of Medicine at Mount Sinai, 1425 Madison Avenue, New York, NY 10029, USA. sophia.frangou@mssm.edu. (S. Frangou).

Contributors

Won Hee Lee and Gaelle Doucet performed neuroimaging data analysis. Sophia Frangou was in charge of study design and implementation including data collection, analysis and interpretation. Evan Leibu oversaw recruitment and clinical evaluation. All authors contributed to manuscript preparation.

Conflict of interest

The authors declare no conflicts of interest in relation to the work described.

Appendix A. Supplementary data

Supplementary data to this article can be found online at https://doi.org/10.1016/j.schres.2018.04.029.

Keywords

Metastability; Synchrony; Kuramoto order parameter; Psychosis; Negative symptoms; Functional connectivity

1. Introduction

Schizophrenia is a neuropsychiatric syndrome associated with disturbances in perception, emotion and cognition (APA, 2013). Multiple genetic, epigenetic, transcriptional and synaptic mechanisms have been implicated in the pathophysiology of schizophrenia (Lewis and Sweet, 2009; Schizophrenia Working Group of the Psychiatric Genomics Consortium, 2014; Glessner et al., 2010; Akbarian, 2014) all of which ultimately impact on the integrity of brain organization. Brain functional organization is characterised by the presence of resting-state networks (RSNs) (Doucet et al., 2011; Fox and Raichle, 2007; van den Heuvel and Hulshoff Pol, 2010; Power et al., 2011) that are defined by the temporal dependency of the spontaneous fluctuations in regional blood-oxygen-level dependent (BOLD) signals (Biswal et al., 1995; Cordes et al., 2000). Functionally, RSNs can be considered in terms of higher-order networks (e.g., default mode, salience) that are involved in sustaining diverse and complex mental operations over time and lower-order networks (e.g., auditory, visual) that rapidly respond to specialized external inputs (Power et al., 2011; Smith et al., 2009).

Dysconnectivity in brain networks is currently the best-supported model for schizophrenia (Frangou, 2014; Stephan et al., 2009; Friston, 1999; Bullmore et al., 1997). Significant disruption in functional connectivity has been demonstrated in multiple RSNs (Pettersson-Yeo et al., 2011; Fornito et al., 2012; Karbasforoushan and Woodward, 2012; Fitzsimmons et al., 2013; Kuhn and Gallinat, 2013; Kambeitz et al., 2015; Dong et al., 2017). The most consistent findings support a general pattern of reduced network cohesion coupled with aberrant integration (Cole et al., 2011; Garrity et al., 2007; Whitfield-Gabrieli et al., 2009; Woodward et al., 2011; Palaniyappan and Liddle, 2012; Venkataraman et al., 2012; Yu et al., 2012; Du et al., 2016; van de Ven et al., 2017; Alderson-Day et al., 2016; Northoff and Qin, 2011; Khadka et al., 2013; Shinn et al., 2013; Kaufmann et al., 2015). There is some evidence that dysconnectivity of the default mode (DMN), central executive (CEN) and salience (SAL) networks is associated with the severity of positive symptoms (Rotarska-Jagiela et al., 2010; Woodward et al., 2011; Khadka et al., 2013; Palaniyappan et al., 2013). However, there remains a significant knowledge gap regarding the association between the disrupted RSN connectivity and the clinical symptoms of schizophrenia.

More recently, the characterisation of the brain functional organization at rest has shifted towards measures that attempt to capture dynamic network properties based on the temporal patterns of the oscillatory activity of their constituent brain regions (Cabral et al., 2011; Deco et al., 2011). Particular attention is focused on network synchrony and metastability. This is because synchrony in the oscillatory activity of network regions is thought to underpin information exchange (Fries, 2005), while metastability represents the variability in the synchronization of network regions over time that is considered important for adaptive information processing (Kelso, 2012; Tognoli and Kelso, 2014). The biological mechanisms

that support these dynamic network properties occur at multiple timescales which also include the slow frequencies measured with functional magnetic resonance imaging (fMRI). We have previously shown that the RSNs differ in metastability in a manner related to the repertoire of network state required for their functional roles (Lee and Frangou, 2017). Higher-order RSNs appear to have lower metastability aligned with their function in sustaining mental operations over time while lower-order RSNs show higher metastability, suggestive of greater capacity to respond quickly to external demands (Lee and Frangou, 2017). The role of metastability in schizophrenia remains unclear; this represents a further knowledge gap in the comprehensive characterisation of schizophrenia-related dysconnectivity despite its potential to provide novel mechanistic insights.

In the present study, we aimed to address the knowledge gaps outlined above using resting-state fMRI data obtained from patients with schizophrenia ($n = 85$) and health individuals ($n = 48$). Based on their involvement in schizophrenia, seven RSNs (default mode, central executive, salience, language, auditory, visual and sensorimotor) were selected for analysis and characterised in terms of their cohesiveness (within-network functional connectivity) and integration (between-network functional connectivity). Based on our previous work (Lee and Frangou, 2017), the synchrony and metastability of each RSN were computed using the Kuramoto order parameter (Shanahan, 2010; Cabral et al., 2011). First, we investigated schizophrenia-related abnormalities in the synchrony and metastability of the selected RSNs. Our main prediction was that schizophrenia-related abnormalities in these dynamic network measures will be primarily observed for the salience network which has emerged as central to the process through which symptoms may emerge (Palaniyappan et al., 2013; Menon, 2011). Further, we tested the explanatory power of the functional connectivity and dynamic features of the RSNs for the symptom dimensions of schizophrenia.

2. Materials and methods

2.1. Participants

The study sample comprised 93 patients with recent onset schizophrenia (illness duration <5 years) and 50 healthy individuals (Table 1). Patients fulfilled criteria for schizophrenia as defined by the fifth edition of the Diagnostic and Statistical Manual of Mental Disorders (DSM-5) (APA, 2013) and were recruited via clinician referrals from the psychiatric services of the Mount Sinai Health System, New York. Healthy individuals were recruited via advertisements in the local press. All participants were screened to exclude those with IQ < 70, medical or neurological disorders, history of significant head trauma, and lifetime history of DSM-5 substance use disorder. The diagnostic status of all participants was determined using the research version of the Structured Clinical interview for DSM-5 (First et al., 2015) supplemented by information from medical records in the case of patients. The presence and severity of psychopathology were assessed in all participants using the expanded 24-item Brief Psychotic Rating Scale (BPRS) (Lukoff et al., 1986) which allows decomposition of the clinical profile of psychosis into four dimensions comprising positive symptoms, negative symptoms, anxiety/depression and agitation/disorganization (Ventura et al., 2000; Kopelowicz et al., 2008). An estimate of IQ was obtained from all participants using the Wechsler Abbreviated Scale of Intelligence, 2nd Edition (WASI-II) (Wechsler,

2011). Medication type and dose was recorded in all patients and the daily antipsychotic dose was converted to chlorpromazine equivalents (CPZE) (Gardner et al., 2010). The study was approved by the Institutional Review Board of the Icahn School of Medicine at Mount Sinai (ISMMS). All participants provided written informed consent.

2.2. Neuroimaging data acquisition and quality assurance

Anatomical and resting-state fMRI (eyes open) data were acquired on a Siemens Skyra 3 T scanner (Erlangen, Germany) at the ISMMS (details in Supplementary Material). Data from the participants were preprocessed using established procedures implemented in Statistical Parametric Mapping software (SPM12; http://www.fil.ion.ucl.ac.uk/spm/software/spm12) and the Data Processing Assistant for Resting-State fMRI software (DPARSF) (Chao-Gan and Yu-Feng, 2010) available in the Data Processing and Analysis for Brain Imaging (DPABI) Toolbox (Yan et al., 2016) (details in Supplementary Material). Two healthy individuals and 8 patients with schizophrenia were excluded because of excessive head motion (linear shift >3 mm or rotation >1° across the run and on a frame-to-frame basis). After removal of these datasets, comparison between groups (patients, healthy volunteers) on multiple head motion parameters (i.e., mean and maximum scan-to-scan head motion and framewise displacement) did not yield significant difference (all $p > 0.05$; details in Supplementary Material).

2.3. Computation of RSN functional connectivity

In each individual resting-state fMRI dataset, we defined seven major RSNs comprising the default mode network (DMN), the central executive network (CEN), the salience network (SAL), the sensorimotor network (SMN), the visual network (VN), the auditory network (AN), and the language network (LAN). These RSNs were defined using validated network masks that are publicly available through the Functional Imaging of Neuropsychiatric Disorders (FIND) Lab, Stanford University (http://findlab.stanford.edu/functional_ROIs.html) (Shirer et al., 2012). Each of the 7 RSN masks comprises its corresponding functional regions-of-interest (ROIs) (Fig. 1A; Supplemental Table S1). We chose functionally defined RSN masks because they offer great cogency and reproducibility (Smith et al., 2009; Laird et al., 2011; Power et al., 2011). We have previously demonstrated the reproducibility of the FIND Lab masks using data from the Human Connectome Project (detailed in Supplemental Material and in Doucet et al., 2018). The median overlap between functionally defined RSN masks (Shirer et al., 2012) and data-driven RSNs (Doucet et al., 2018) was 91%. We assessed the cohesiveness and integration of each RSN by computing their within-and between-network functional connectivity. Within-network functional connectivity was estimated by averaging the fMRI time series over all the voxels within each network region and then calculating all possible pairwise Pearson's correlation between the network regions. Between-network functional connectivity was estimated by computing pairwise Pearson's correlation between the networks' average time series. All correlation coefficients were transformed into Fisher's z-score prior to further analyses. These computations resulted in 28 connectivity measures per subject which were used in further analyses. No correlation was found between any of these measures and framewise displacement (FD) even at $p < 0.05$, uncorrected (detailed in Supplementary Material).

2.4. Computation of network synchrony and metastability

The voxel-wise BOLD data for each RSN were filtered to extract frequency-band fMRI signals using the maximal overlap discrete wavelet transform (MODWT) (Percival and Walden, 2000). Because the repetition time of the fMRI data acquisition was 1 s, the frequency bands extracted were: scale 1 = 0.25–0.5 Hz; scale 2 = 0.13–0.25 Hz; scale 3 = 0.06–0.13 Hz; scale 4 = 0.03–0.06 Hz; scale 5 = 0.015–0.03 Hz. We used a wavelet filter of Daubechies Least Asymmetric with a wavelet length of 8 (Lee and Frangou, 2017). We focused on scale 4 wavelet coefficients, because the most relevant information for resting-state fMRI data is mainly contained within this scale (Achard et al., 2006; Biswal et al., 1995; Fornito et al., 2010; Glerean et al., 2012). We then extracted the phases of the fMRI time series for each RSN in each participant by applying the Hilbert transform to the wavelet-filtered fMRI BOLD signals to obtain the associated analytical signals. The analytic signal represents a narrowband signal, $s(t)$, in the time domain as a rotating vector with an instantaneous phase, φ(t), and an instantaneous amplitude, $A(t)$, i.e., $s(t) = A(t)\cos(\varphi(t))$. The phase and the amplitude are given by the argument and the modulus, respectively, of the complex signal $z(t)$, given by $z(t) = s(t) + i\mathrm{H}[s(t)]$, where i is the imaginary unit and $\mathrm{H}[s(t)]$ is the Hilbert transform of $s(t)$ (Glerean et al., 2012; PonceAlvarez et al., 2015). Subsequently, the first and last 10 time steps were discarded to avoid border effect inherent to the Hilbert transform (Ponce-Alvarez et al., 2015). To evaluate the dynamic properties of each RSN, we computed the Kuramoto order parameter $R(t)$, defined as

$$R(t) = \left| \frac{1}{N} \sum_{n=1}^{N} e^{i\varphi_n(t)} \right|$$

where N is the total number of voxels within each RSN and $\varphi_n(t)$ is the instantaneous phase of each fMRI BOLD signal at voxel n of each RSN. This parameter measures the level of synchronization between brain regions across time (Fig. 1B). For each network, synchrony (mean synchronization) and metastability (the variation in synchronization over time) were defined as the mean and the standard deviation of the Kuramoto order parameter over time, respectively (Cabral et al., 2011; Lee et al., 2017; Shanahan, 2010; Váša et al., 2015). These computations resulted in 14 measures per subject that were used in further analyses.

2.5. Statistical analysis

Group differences in demographic characteristics and IQ were examined using t- and χ^2 tests as appropriate. We detected an effect of group for sex and IQ and we therefore conducted collinearity diagnostics using regression models. These variables were not collinear as their variance inflation factor (VIF) ranged between 1 and 1.4 which is below the traditional threshold of 2 for collinearity. We performed three multivariate analyses of covariance (MANOVAs) to examine the effect of diagnosis separately on measures of network dynamics (synchrony and metastability), measures of within-network functional connectivity and measures of between-network functional connectivity. Sex and IQ were entered as covariates in all analyses. For each MANOVA, when the overall model was significant at $p < 0.05$, we conducted post-hoc pairwise comparisons for which the threshold of statistical significance was adjusted using Bonferroni correction based on the number of

variables included in each model. In addition, the effect size of case-control differences in neuroimaging measures was calculated using the Cohen's *d* (Nakagawa and Cuthill, 2007). The predictive value of the neuroimaging variables for clinical symptoms was only tested in the patient group. The four BPRS symptom scores were not collinear ($|r| < 0.4$) and were used as dependent factors in separate stepwise regression analyses. This approach operates by successively adding and removing predictor variables based on their squared t-statistic to select the best grouping of predictor variables that accounts for most of the variance (R^2) in the outcome. The assumptions, advantages and limitations of this approach are well understood (e.g. Derksen and Keselman, 1992; Burnham and Anderson, 2002; Cohen et al., 2013). Stepwise regression models allow a principled and data-driven selection of predictor variables, that is largely independent of sample size, and are best suited for testing prespecified hypotheses about the predictor and outcome variables. This is the case here as our aim was to test the predictive value of predefined connectivity features for symptom severity in schizophrenia. Stepwise regression analyses are prone to R^2 values inflation and are sensitive to the presence of collinearity amongst the predictor variables. To address these concerns, we undertook the following three steps: (a) Curve estimation and collinearity assessments were conducted to select the neuroimaging variables entered as independent predictors. Variables were considered co-linear if their pairwise correlation was $|r| > 0.4$. The synchrony and metastability of each network were the only highly correlated (r values ranged between 0.63 and 0.72) neuroimaging variables and therefore only metastability was entered in the regression analyses. (b) We confirmed that none of the regression results showed collinearity based on VIF <2 and tolerance >0.2. (c) We examined the reliability of the R^2 values of the regression models using a leave-one-out method that enables testing the reliability of these values while preserving statistical power.

3. Results

The descriptive statistics for all neuroimaging parameters are shown in Supplemental Table S2 and univariate correlations between neuroimaging measures and symptom dimensions are shown in Supplemental Figs. S1 and S2. None of the neuroimaging parameters showed significant correlations with medication dose expressed in daily CPZE (all |ρ| b 0.17, $p >$ 0.07, uncorrected).

3.1. Effect of diagnosis on network dynamic and connectivity measures

The effect size of the case-control differences for within- and between-network functional connectivity, network metastability and synchrony are shown in Supplemental Table S2. We found a significant effect of diagnosis on the dynamic network measures ($F_{14,113} = 1.91$; $p =$ 0.03). There was no significant effect of sex ($F_{14,113} = 0.12$; $p = 0.35$) or IQ ($F_{14,113} = 0.11$; $p = 0.37$). No interactions were significant either ($p > 0.05$). Post-hoc pairwise comparisons showed that the SAL network had higher metastability ($p = 0.042$, Bonferroni corrected) and synchrony ($p = 0.028$, Bonferroni corrected) in patients than healthy participants. We also found a significant effect of diagnosis on the within-network functional connectivity ($F_{7,122}$ = 2.11; $p = 0.04$). There were no other significant effects (sex: $F_{7,122} = 1.35$; $p = 0.23$; IQ: $F_{7,122} = 1.14$; $p = 0.34$) or interactions ($p > 0.05$). Post-hoc pairwise comparisons showed that the SAL within-network connectivity was higher in patients than healthy participants (*p*

= 0.024, uncorrected) although this finding was below the Bonferroni-adjusted threshold. The multivariate analysis of covariation for between-network functional connectivity did not reach statistical significance for diagnosis ($F_{19,109} = 1.53$; $p = 0.08$), sex ($F_{19,109} = 1.50$; $p = 0.11$) or IQ ($F_{19,109} = 1.08$; p = 0.37). The effect of diagnosis remained below the conventional threshold for statistical significance ($F_{19,113} = 1.59$; $p = 0.06$) even after removing the covariates.

3.2. Neuroimaging predictors of symptom dimensions in schizophrenia

3.2.1. Positive symptoms—The best model explained 14% of the variance in symptom severity (Table 2; Supplementary Fig. S3). Measures of functional connectivity between the DMN-SMN, DMN-CEN and SMN-AN made a statistically significant contribution to the model, such that for any unit increase in the connectivity between these networks, the model predicted lower BPRS positive symptom score (Table 2, Fig. 2).

3.2.2. Negative symptoms—The best model explained 17% of the variance in symptom severity (Table 2). The neuroimaging variables that made a statistically significant contribution to the model were the metastability and within-network connectivity of the SAL network and the connectivity between AN-LAN. For each unit increase in SAL metastability and in AN-LAN connectivity, the model predicted higher BPRS negative symptom score while for any unit increase in the within-network connectivity of the SAL network, the model predicted lower BPRS negative symptom score (Table 2, Fig. 2).

3.2.3. Anxiety/depression—The best model explained 12% of the variance in symptom severity (Table 2). The neuroimaging variables that made a statistically significant contribution to the model were the within-network connectivity of the SAL and the connectivity between SAL-LAN and SMN-AN. For any unit increase in any of these connectivity measures, the model predicted lower scores in BPRS anxiety/depression symptoms (Table 2, Fig. 2).

3.2.4. Agitation/disorganization—The best model explained 5% of the variance in agitation/disorganization (Table 2). Only the connectivity between SAL-CEN made a statistically significant contribution such that increased connectivity between these networks predicted higher BPRS agitation/disorganization scores (Table 2, Fig. 2).

4. Discussion

The present study evaluated the explanatory value of fMRI-derived measures of RSN functional organization for the symptoms of schizophrenia. Importantly, we did not limit our investigation to positive symptoms. Instead, we considered the entire spectrum of psychopathology in schizophrenia in accordance with previous studies which have shown that positive symptoms, amotivation/negative symptoms, depressive/anxious symptoms and agitation/disorganization represent separable factors (Peralta et al., 2013; Russo et al., 2014). This factor structure is present at the first psychotic episode; it is longitudinally stable (Russo et al., 2014) and is captured by the BPRS (Lukoff et al., 1986). Our results provide further empirical support to the notion that brain dysconnectivity underlies symptomatic expression in schizophrenia. The parameters of RSN functional organization considered here

explained a sizable proportion of the variance in symptom severity with the exception of disorganization.

To our knowledge, this is the first study on RSN synchrony and metastability in schizophrenia and the results reinforce the importance of the SAL network. The SAL network is anchored in the anterior insula and dorsal anterior cingulate cortex and has prominent prefrontal, limbic and subcortical connections (Seeley et al., 2007). It is widely accepted that the primary function of this network is to integrate sensory, visceral and affective data in order to direct attention and shape cognitive and behavioral responses (Seeley et al., 2007; Sridharan et al., 2008; Medford and Critchley, 2010; Menon and Uddin, 2010). Meta-analyses of neuroimaging studies in schizophrenia have reported reductions in the volume of the constituent regions of the SAL network (Haijma et al., 2013), in its internal coherence and its integration within the brain functional connectome (Dong et al., 2017). It has been proposed that the SAL network disruption impairs the appropriate attribution of salience to internal and external events and leads to reality distortion (Menon, 2011; Northoff and Qin, 2011; Alderson-Day et al., 2016) and to anxious/depressive symptoms (Kaiser et al., 2015). Disruption in the SAL network may also contribute to negative symptoms as difficulties in allocating motivational salience and initiating appropriate responses may present as lack of motivation and reduced emotional responsivity (Menon, 2011). The results of this study partly confirmed these predictions as parameters of the SAL functional organization contributed to negative, anxious/depressive and disorganization symptoms.

Importantly, the findings of this study offer novel putative mechanistic insights into the SAL network dysfunction in schizophrenia based on the dynamic features of the network. Synchrony between network regions is required for the exchange of information; the degree of synchrony and its variability (i.e., metastability) over time define different network states; weakly synchronized states are dominated by noise while highly synchronized states prevent information flow (Fries, 2005; Kelso, 2012; Tognoli and Kelso, 2014). The increase in SAL network synchrony in patients compared to healthy participants implies impediments in the propagation of salience-related information within the network. The metastability of the SAL network was also increased, indicating greater variability in SAL network states in patients. This finding could be interpreted as a reduction in the capacity of the SAL network to maintain contextually-appropriate network states but may also indicate abnormally increased flexibility of the SAL network that allows it to adopt contextually-inappropriate configurations. Future work involving a broad-range of behavioral and cognitive tasks in the scanner will be required to better characterize the patterns of impairment in salience monitoring and allocation associated with altered SAL network synchrony and metastability in schizophrenia. We also note that changes in metastability and synchronyof moderate effect size were also present in patients in the VN, AN, and LAN networks. These initial results underscore the value of larger studies on network dynamics in schizophrenia.

The DMN integration emerged as the primary contributor to positive symptoms. The DMN is implicated in self-referential and integrative processes that do not require attention to external stimuli or events (Raichle et al., 2001; Greicius et al., 2003). In the current study, greater functional integration of the DMN with the CEN and SMN predicted lower positive

symptom severity. Abnormalities in the functional integration of the SMN are likely to disrupt the orderly processing of sensorimotor information and may thus contribute to reality distortion. The CEN is involved in goal-directed and task-related selection of stimuli and responses (Corbetta and Shulman, 2002). The two networks typically have an antagonistic relationship and a successful suppression of the DMN by the CEN is considered crucial for optimal cognitive task performance (Sridharan et al., 2008).

Of note, higher integration between the SMN-AN predicted lower severity for positive symptoms. This finding is aligned with the impaired corollary discharge (or efference copy) hypothesis of schizophrenia which posits that positive psychotic symptoms reflect impairment in somatosensory and auditory integration (Feinberg, 1978; Frith et al., 2000; Mathalon and Ford, 2008). These corollary signals accompany motor action and enable prediction of the sensory consequences of self-initiated action and thus their differentiation from externally triggered events (Von Holst and Mittelstaedt, 1950; Sperry, 1950; Blakemore et al., 1998). Multisensory prediction deficits in schizophrenia, and their relation to hallucinations and delusions, have been reported in multiple electrophysiological and imaging studies (Ford and Mathalon, 2012; Picard and Friston, 2014; Shergill et al., 2014).

In addition to its association with positive symptoms, greater SMN-AN integration also predicted lower levels of anxious/depressive symptoms. This observation is relevant to on-going debates about the association between multisensory prediction errors, positive symptoms and anxious/depressive symptoms. It has been suggested that multisensory prediction errors giving rise to positive symptoms may also trigger distress and depression either because of their unpredictable nature (Gallagher, 2005; Fletcher and Frith, 2009) but also because they often have unpleasant, persecutory and derogatory content (Kjelby et al., 2015). Conversely, heighted levels of anxiety/depression may give rise to multisensory prediction errors since such feelings often precede the onset or recurrence of positive symptoms (Freeman and Garety, 2003; Allen et al., 2005).

Some limitations to this work should be noted. First, the sample size was moderate and we may have restricted power to detect some effects, particularly in connection to network dynamics and integration (Supplemental Table S1). At the same time, those findings that were statistically significant are likely to reflect core pathophysiological processes. Moreover, we provided the first estimates of the effect size of casecontrol differences in RSN synchrony and metastability that would be useful in guiding future study design in schizophrenia. Second, the two diagnostic groups were not matched for sex. Analyses of large fMRI datasets have shown that sex is relevant for resting-state functional connectivity (e.g., Biswal et al., 2010) but not for synchrony or metastability (Lee and Frangou, 2017; Lee et al., 2018). In any case, sex did not make any statistically significant contribution to the results of the current study. Third, we used masks to define the RSNs in preference to other methods for partitioning the resting-state connectome. The most widely used alternative is independent component analysis. This approach may be more sensitive to individual-level variability but functionally defined masks such as the one employed here have the advantage of greater cogency and reproducibility (Laird et al. 2011; Smith et al., 2009; Power et al., 2011; Doucet et al., 2011). Fourth, the severity of the clinical symptoms varies across samples and within the same patient over time. The patients included in this

study were in the early stages of the disorder and were selected to minimize potential confounders associated with chronicity. Confirmation of the robustness of our findings requires replication in larger samples and in longitudinal studies. Fifth, medication status was based on patients' self-report and on information from medical records regarding their prescriptions. The majority of patients were on regular antipsychotic medication. Although the daily antipsychotic dose did not correlate with any neuroimaging measure, the effect of medication cannot be conclusively excluded.

Overall, the results reported here demonstrate that abnormalities in RSN connectivity and metastability explain a significant proportion of the symptom dimensions of schizophrenia. They also reinforce the importance of the SAL network for schizophrenia and point to novel mechanisms that may explain the abnormalities in salience processing observed in schizophrenia.

Supplementary Material

Refer to Web version on PubMed Central for supplementary material.

Acknowledgments

This work was supported by the National Institute of Mental Health under grant R01MH104284.

Role of funding source

None of the funders influenced the conduct of the study or the interpretation and presentation of the results.

References

Achard S, Salvador R, Whitcher B, Suckling J, Bullmore E, 2006 A resilient, low-frequency, small-world human brain functional network with highly connected association cortical hubs. J. Neurosci. 26 (1), 63–72. [PubMed: 16399673]

Akbarian S, 2014 Epigenetic mechanisms in schizophrenia. Dialogues Clin. Neurosci. 16 (3), 405–417. [PubMed: 25364289]

Alderson-Day B, Diederen K, Fernyhough C, Ford JM, Horga G, Margulies DS, McCarthy-Jones S, Northoff G, Shine JM, Turner J, van de Ven V, van Lutterveld R, Waters F, Jardri R, 2016 Auditory hallucinations and the Brain's resting-state networks: findings and methodological observations. Schizophr. Bull. 42 (5), 1110–1123. [PubMed: 27280452]

Allen P, Freeman D, McGuire P, Garety P, Kuipers E, Fowler D, Bebbington P, Green C, Dunn G, Ray K, 2005 The prediction of hallucinatory predisposition in nonclinical individuals: examining the contribution of emotion and reasoning. Br. J. Clin. Psychol 44 (Pt 1), 127–132. [PubMed: 15826349]

American Psychiatric Association, 2013 Diagnostic and Statistical Manual of Mental Disorders: DSM-5. American Psychiatric Association, Washington, D.C.

Biswal B, Yetkin FZ, Haughton VM, Hyde JS, 1995 Functional connectivity in the motor cortex of resting human brain using echo-planar MRI. Magn. Reson. Med 34 (4), 537–541. [PubMed: 8524021]

Biswal BB, Mennes M, Zuo XN, Gohel S, Kelly C, Smith SM, Beckmann CF, Adelstein JS, Buckner RL, Colcombe S, Dogonowski AM, Ernst M, Fair D, Hampson M, Hoptman MJ, Hyde JS, Kiviniemi VJ, Kötter R, Li SJ, Lin CP, Lowe MJ, Mackay C, Madden DJ, Madsen KH, Margulies DS, Mayberg HS, McMahon K, Monk CS, Mostofsky SH, Nagel BJ, Pekar JJ, Peltier SJ, Petersen SE, Riedl V, Rombouts SA, Rypma B, Schlaggar BL, Schmidt S, Seidler RD, Siegle GJ, Sorg C, Teng GJ, Veijola J, Villringer A, Walter M, Wang L, Weng XC, Whitfield-Gabrieli S, Williamson P,

Windischberger C, Zang YF, Zhang HY, Castellanos FX, Milham MP, 2010 Toward discovery science of human brain function. Proc. Natl. Acad. Sci. U. S. A 107 (10), 4734–4739. [PubMed: 20176931]

Blakemore S, Rees G, Frith C, 1998 How do we predict the consequences of our actions? A functional imaging study. Neuropsychologia 36 (6), 521–529. [PubMed: 9705062]

Bullmore ET, Frangou S, Murray RM, 1997 The dysplastic net hypothesis: an integration of developmental and dysconnectivity theories of schizophrenia. Schizophr. Res. 28 (2–3), 143–156. [PubMed: 9468349]

Burnham KP, Anderson DR, 2002 Model Selection and Multimodel Inference: a Practice Information-theoretic Approach. Springer Verlag, New York.

Cabral J, Hugues E, Sporns O, Deco G, 2011 Role of local network oscillations in resting-state functional connectivity. NeuroImage 57 (1), 130–139. [PubMed: 21511044]

Chao-Gan Y, Yu-Feng ZDPARSF, 2010 A MATLAB toolbox for "pipeline" data analysis of resting-state fMRI. Front. Syst. Neurosci 14 (4), 13.

Cohen J, Cohen P, West SG, Aiken LS, 2013 Applied Multiple Regression/correlation Analysis for the Behavioral Sciences. Routledge.

Cole MW, Anticevic A, Repovs G, Barch D, 2011 Variable global dysconnectivity and individual differences in schizophrenia. Biol. Psychiatry 70 (1), 43–50. [PubMed: 21496789]

Corbetta M, Shulman GL, 2002 Control of goal-directed and stimulus-driven attention in the brain. Nat. Rev. Neurosci 3 (3), 201–215. [PubMed: 11994752]

Cordes D, Haughton VM, Arfanakis K, Wendt GJ, Turski PA, Moritz CH, Quigley MA, Meyerand ME, 2000 Mapping functionally related regions of brain with functional connectivity MR imaging. AJNR Am. J. Neuroradiol 21 (9), 1636–1644. [PubMed: 11039342]

Deco G, Jirsa VK, McIntosh AR, 2011 Emerging concepts for the dynamical organization of resting-state activity in the brain. Nat. Rev. Neurosci 12 (1), 43–56. [PubMed: 21170073]

Derksen S, Keselman HJ, 1992 Backward, forward and stepwise automated subset selection algorithms: frequency of obtaining authentic and noise variables. Br. J. Math. Stat. Psychol 45 (2), 265–282.

Dong D, Wang Y, Chang X, Luo C, Yao D, 2017 Dysfunction of large-scale brain networks in schizophrenia: a meta-analysis of resting-state functional connectivity. Schizophr. Bull 10.1093/schbul/sbx034.

Doucet G, Naveau M, Petit L, Delcroix N, Zago L, Crivello F, Jobard G, Tzourio-Mazoyer N, Mazoyer B, Mellet E, Joliot M, 2011 Brain activity at rest: a multiscale hierarchical functional organization. J. Neurophysiol 105 (6), 2753–2763. [PubMed: 21430278]

Doucet GE, Rasgon N, McEwen BS, Micali N, Frangou S, 2018 Elevated body mass index is associated with increased integration and reduced cohesion of sensorydriven and internally guided resting-state functional brain networks. Cereb. Cortex 28 (3), 988–997. [PubMed: 28119342]

Du Y, Pearlson GD, Yu Q, He H, Lin D, Sui J, Wu L, Calhoun VD, 2016 Interaction among subsystems within default mode network diminished in schizophrenia patients: a dynamic connectivity approach. Schizophr. Res 170 (1), 55–65. [PubMed: 26654933]

Feinberg I, 1978 Efference copy and corollary discharge: implications for thinking and its disorders. Schizophr. Bull. 4 (4), 636–640. [PubMed: 734369]

First MB, Williams JBW, Karg RS, Spitzer RL, 2015 Structured Clinical Interview for DSM-5-Research Version. American Psychiatric Association, Arlington, VA.

Fitzsimmons J, Kubicki M, Shenton ME, 2013 Review of functional and anatomical brain connectivity findings in schizophrenia. Curr. Opin. Psychiatry 26 (2), 172–187. [PubMed: 23324948]

Fletcher PC, Frith CD, 2009 Perceiving is believing: a Bayesian approach to explaining the positive symptoms of schizophrenia. Nat. Rev. Neurosci 10 (1), 48–58. [PubMed: 19050712]

Ford JM, Mathalon DH, 2012 Anticipating the future: automatic prediction failures in schizophrenia. Int. J. Psychophysiol 83 (2), 232–239. [PubMed: 21959054]

Fornito A, Zalesky A, Bullmore ET, 2010 Network scaling effects in graph analytic studies of human resting-state FMRI data. Front. Syst. Neurosci 4, 22. [PubMed: 20592949]

Fornito A, Zalesky A, Pantelis C, Bullmore ET, 2012 Schizophrenia, neuroimaging and connectomics. NeuroImage 62 (4), 2296–2314. [PubMed: 22387165]

Fox MD, Raichle ME, 2007 Spontaneous fluctuations in brain activity observed with functional magnetic resonance imaging. Nat. Rev. Neurosci 8 (9), 700–711. [PubMed: 17704812]

Frangou S, 2014 A systems neuroscience perspective of schizophrenia and bipolar disorder. Schizophr. Bull 40 (3), 523–531. [PubMed: 24609453]

Freeman D, Garety PA, 2003 Connecting neurosis and psychosis: the direct influence of emotion on delusions and hallucinations. Behav. Res. Ther 41 (8), 923–947. [PubMed: 12880647]

Fries P, 2005 A mechanism for cognitive dynamics: neuronal communication through neuronal coherence. Trends Cogn. Sci 9 (2), 474–480. [PubMed: 16150631]

Friston KJ, 1999 Schizophrenia and the disconnection hypothesis. Acta Psychiatr. Scand. Suppl 395, 68–79. [PubMed: 10225335]

Frith CD, Blakemore S, Wolpert DM, 2000 Explaining the symptoms of schizophrenia: abnormalities in the awareness of action. Brain Res. Brain Res. Rev 31 (2–3), 357–363. [PubMed: 10719163]

Gallagher S, 2005 How the Body Shapes the Mind. Oxford University Press, Oxford.

Gardner DM, Murphy AL, O'Donnell H, Centorrino F, Baldessarini RJ, 2010 International consensus study of antipsychotic dosing. Am. J. Psychiatry 167 (6), 686–693. [PubMed: 20360319]

Garrity AG, Pearlson GD, McKiernan K, Lloyd D, Kiehl KA, Calhoun VD, 2007 Aberrant "default mode" functional connectivity in schizophrenia. Am. J. Psychiatry 164 (3), 450–457. [PubMed: 17329470]

Glerean E, Salmi J, Lahnakoski JM, Jaaskelainen IP, Sams M, 2012 Functional magnetic resonance imaging phase synchronization as a measure of dynamic functional connectivity. Brain Connect. 2 (2), 91–101. [PubMed: 22559794]

Glessner JT, Reilly MP, Kim CE, Takahashi N, Albano A, Hou C, Bradfield JP, Zhang H, Sleiman PM, Flory JH, Imielinski M, Frackelton EC, Chiavacci R, Thomas KA, Garris M, Otieno FG, Davidson M, Weiser M, Reichenberg A, Davis KL, Friedman JI, Cappola TP, Margulies KB, Rader DJ, Grant SF, Buxbaum JD, Gur RE, Hakonarson H, 2010 Strong synaptic transmission impact by copy number variations in schizophrenia. Proc. Natl. Acad. Sci. U. S. A 107 (23), 10584–10589. [PubMed: 20489179]

Greicius MD, Krasnow B, Reiss AL, Menon V, 2003 Functional connectivity in the resting brain: a network analysis of the default mode hypothesis. Proc. Natl. Acad. Sci. U. S. A 100 (1), 253–258. [PubMed: 12506194]

Haijma SV, Van Haren N, Cahn W, Koolschijn PC, Hulshoff Pol HE, Kahn RS, 2013 Brain volumes in schizophrenia: a meta-analysis in over 18 000 subjects. Schizophr. Bull 39 (5), 1129–1138. [PubMed: 23042112]

Kaiser RH, Andrews-Hanna JR, Wager TD, Pizzagalli DA, 2015 Large-scale network dysfunction in major depressive disorder: a meta-analysis of resting-state functional connectivity. JAMA Psychiatry 72 (6), 603–611. [PubMed: 25785575]

Kambeitz J, Kambeitz-Ilankovic L, Leucht S, Wood S, Davatzikos C, Malchow B, Falkai P, Koutsouleris N, 2015 Detecting neuroimaging biomarkers for schizophrenia: a meta-analysis of multivariate pattern recognition studies. Neuropsychopharmacology 40 (7), 1742–1751. [PubMed: 25601228]

Karbasforoushan H, Woodward ND, 2012 Resting-state networks in schizophrenia. Curr. Top. Med. Chem 12 (21), 2404–2414. [PubMed: 23279179]

Kaufmann T, Skåtun KC, Alnæs D, Doan NT, Duff EP, Tønnesen S, Roussos E, Ueland T, Aminoff SR, Lagerberg TV, Agartz I, Melle IS, Smith SM, Andreassen OA, Westlye LT, 2015 Disintegration of sensorimotor brain networks in schizophrenia. Schizophr. Bull 41 (6), 1326–1335. [PubMed: 25943122]

Kelso JA, 2012 Multistability and metastability: understanding dynamic coordination in the brain. Philos. Trans. R. Soc. Lond. Ser. B Biol. Sci 367, 906–918. [PubMed: 22371613]

Khadka S, Meda SA, Stevens MC, Glahn DC, Calhoun VD, Sweeney JA, Tamminga CA, Keshavan MS, O'Neil K, Schretlen D, Pearlson GD, 2013 Is aberrant functional connectivity a psychosis endophenotype? A resting state functional magnetic resonance imaging study. Biol. Psychiatry 74 (6), 458–466. [PubMed: 23746539]

Kjelby E, Sinkeviciute I, Gjestad R, Kroken RA, Løberg EM, Jørgensen HA, Hugdahl K, Johnsen E, 2015 Suicidality in schizophrenia spectrum disorders: the relationship to hallucinations and persecutory delusions. Eur. Psychiatry 30 (7), 830–836. [PubMed: 26443050]

Kopelowicz A, Ventura J, Liberman RP, Mintz J, 2008 Consistency of brief psychiatric scale factor structure across a broad spectrum of schizophrenia patients. Psychopathology 41 (2), 77–84. [PubMed: 18033976]

Kuhn S, Gallinat J, 2013 Resting-state brain activity in schizophrenia and major depression: a quantitative meta-analysis. Schizophr. Bull 39 (2), 358–365. [PubMed: 22080493]

Laird AR, Fox PM, Eickhoff SB, Turner JA, Ray KL, McKay DR, Glahn DC, Beckmann CF, Smith SM, Fox PT, 2011 Behavioral interpretations of intrinsic connectivity networks. J. Cogn. Neurosci 23 (12), 4022–4037. [PubMed: 21671731]

Lee WH, Frangou S, 2017 Linking functional connectivity and dynamic properties of resting-state networks. Sci. Rep. 7 (1), 16610. [PubMed: 29192157]

Lee WH, Bullmore E, Frangou S, 2017 Quantitative evaluation of simulated functional brain networks in graph theoretical analysis. NeuroImage 146, 724–733. [PubMed: 27568060]

Lee WH, Moser DA, Ing A, Doucet GE, Frangou S, 2018 Behavioral and health correlates of resting-state metastability in the human connectome project. Brain Topogr. (in press).

Lewis DA, Sweet RA, 2009 Schizophrenia from a neural circuitry perspective: advancing toward rational pharmacological therapies. J. Clin. Invest 119 (4), 706–716. [PubMed: 19339762]

Lukoff D, Liberman RP, Nuechterlein KH, 1986 Symptom monitoring in the rehabilitation of schizophrenic patients. Schizophr. Bull 12 (4), 578–602. [PubMed: 3810065]

Mathalon DH, Ford JM, 2008 Corollary discharge dysfunction in schizophrenia: evidence for an elemental deficit. Clin. EEG Neurosci 39 (2), 82–86. [PubMed: 18450174]

Medford N, Critchley HD, 2010 Conjoint activity of anterior insular and anterior cingulate cortex: awareness and response. Brain Struct. Funct 214 (5–6), 535–549. [PubMed: 20512367]

Menon V, 2011 Large-scale brain networks and psychopathology: a unifying triple network model. Trends Cogn. Sci 15 (10), 483–506. [PubMed: 21908230]

Menon V, Uddin LQ, 2010 Saliency, switching, attention and control: a network model of insula function. Brain Struct. Funct 214 (5–6), 655–667. [PubMed: 20512370]

Nakagawa S, Cuthill IC, 2007 Effect size, confidence interval and statistical significance: a practical guide for biologists. Biol. Rev. Camb. Philos. Soc 82 (4), 591–605. [PubMed: 17944619]

Northoff G, Qin P, 2011 How can the brain's resting state activity generate hallucinations? A "resting state hypothesis" of auditory verbal hallucinations. Schizophr. Res. 127 (1–3), 202–214. [PubMed: 21146961]

Palaniyappan L, Liddle PF, 2012 Does the salience network play a cardinal role in psychosis? An emerging hypothesis of insular dysfunction. J. Psychiatry Neurosci 37 (1), 17–27. [PubMed: 21693094]

Palaniyappan L, Simmonite M, White TP, Liddle EB, Liddle PF, 2013 Neural primacy of the salience processing system in schizophrenia. Neuron 79 (4), 814–828. [PubMed: 23972602]

Peralta V, Moreno-Izco L, Calvo-Barrena L, Cuesta MJ, 2013 The low- and higherorder factor structure of symptoms in patients with a first episode of psychosis. Schizophr. Res. 147 (1), 116–124. [PubMed: 23582653]

Percival DB, Walden AT, 2000 Wavelet Methods for Time Series Analysis. Cambridge University Press, Cambridge; New York.

Pettersson-Yeo W, Allen P, Benetti S, McGuire P, Mechelli A, 2011 Dysconnectivity in schizophrenia: where are we now? Neurosci. Biobehav. Rev 35 (5), 1110–1124. [PubMed: 21115039]

Picard F, Friston K, 2014 Predictions, perception, and a sense of self. Neurology 83 (12), 1112–1118. [PubMed: 25128179]

Ponce-Alvarez A, Deco G, Hagmann P, Romani GL, Mantini D, Corbetta M, 2015 Resting-state temporal synchronization networks emerge from connectivity topology and heterogeneity. PLoS Comput. Biol 11.

Power JD, Cohen AL, Nelson SM, Wig GS, Barnes KA, Church JA, Vogel AC, Laumann TO, Miezin FM, Schlaggar BL, Petersen SE, 2011 Functional network organization of the human brain. Neuron 72 (4), 665–678. [PubMed: 22099467]

Raichle ME, MacLeod AM, Snyder AZ, Powers WJ, Gusnard DA, Shulman GL, 2001 A default mode of brain function. Proc. Natl. Acad. Sci. U. S. A 98 (2), 676–682. [PubMed: 11209064]

Rotarska-Jagiela A, van de Ven V, Oertel-Knöchel V, Uhlhaas PJ, Vogeley K, Linden DE, 2010 Resting-state functional network correlates of psychotic symptoms in schizophrenia. Schizophr. Res 117 (1), 21–30. [PubMed: 20097544]

Russo M, Levine SZ, Demjaha A, Di Forti M, Bonaccorso S, Fearon P, Dazzan P, Pariante CM, David AS, Morgan C, Murray RM, Reichenberg A, 2014 Association between symptom dimensions and categorical diagnoses of psychosis: a crosssectional and longitudinal investigation. Schizophr. Bull 40 (1), 111–119. [PubMed: 23661632]

Schizophrenia Working Group of the Psychiatric Genomics Consortium, 2014 Biological insights from 108 schizophrenia-associated genetic loci. Nature 511 (7510), 421–427. [PubMed: 25056061]

Seeley WW, Menon V, Schatzberg AF, Keller J, Glover GH, Kenna H, Reiss AL, Greicius MD, 2007 Dissociable intrinsic connectivity networks for salience processing and executive control. J. Neurosci 27 (9), 2349–2356. [PubMed: 17329432]

Shanahan M, 2010 Metastable chimera states in community-structured oscillator networks. Chaos 20, 013108. [PubMed: 20370263]

Shergill SS, White TP, Joyce DW, Bays PM, Wolpert DM, Frith CD, 2014 Functional magnetic resonance imaging of impaired sensory prediction in schizophrenia. JAMA Psychiatry 71 (1), 28–35. [PubMed: 24196370]

Shinn AK, Baker JT, Cohen BM, Öngür D, 2013 Functional connectivity of left Heschl's gyrus in vulnerability to auditory hallucinations in schizophrenia. Schizophr. Res 143 (2–3), 260–268. [PubMed: 23287311]

Shirer WR, Ryali S, Rykhlevskaia E, Menon V, Greicius MD, 2012 Decoding subject-driven cognitive states with whole-brain connectivity patterns. Cereb. Cortex 22 (1), 158–165. [PubMed: 21616982]

Smith SM, Fox PT, Miller KL, Glahn DC, Fox PM, Mackay CE, Filippini N, Watkins KE, Toro R, Laird AR, Beckmann CF, 2009 Correspondence of the brain's functional architecture during activation and rest. Proc. Natl. Acad. Sci. U. S. A 106 (31), 13040–13045. [PubMed: 19620724]

Sperry RW, 1950 Neural basis of the spontaneous optokinetic response produced by visual inversion. J. Comp. Physiol. Psychol 43 (6), 482–489. [PubMed: 14794830]

Sridharan D, Levitin DJ, Menon V, 2008 A critical role for the right fronto-insular cortex in switching between central-executive and default-mode networks. Proc. Natl. Acad. Sci. U. S. A 105 (34), 12569–12574. [PubMed: 18723676]

Stephan KE, Friston KJ, Frith CD, 2009 Dysconnection in schizophrenia: from abnormal synaptic plasticity to failures of self-monitoring. Schizophr. Bull 35 (3), 509–527. [PubMed: 19155345]

Tognoli E, Kelso JA, 2014 The metastable brain. Neuron 81 (1), 35–48. [PubMed: 24411730]

van de Ven V, Rotarska Jagiela A, Oertel-Knöchel V, David EJ, Linden DEJ, 2017 Reduced intrinsic visual cortical connectivity is associated with impaired perceptual closure in schizophrenia. Neuroimage Clin. 15, 45–52. [PubMed: 28480163]

van den Heuvel MP, Hulshoff Pol HE, 2010 Exploring the brain network: a review on resting-state fMRI functional connectivity. Eur. Neuropsychopharmacol 20 (8), 519–534. [PubMed: 20471808]

Váša F, Shanahan M, Hellyer PJ, Scott G, Cabral J, Leech R, 2015 Effects of lesions on synchrony and metastability in cortical networks. NeuroImage 118, 456–467. [PubMed: 26049146]

Venkataraman A, Whitford TJ, Westin CF, Golland P, Kubicki M, 2012 Whole brain resting state functional connectivity abnormalities in schizophrenia. Schizophr. Res. 139 (1–3), 7–12. [PubMed: 22633528]

Ventura J, Nuechterlein KH, Subotnik KL, Gutkind D, Gilbert EA, 2000 12 27 Symptom dimension in recent-onset schizophrenia and mania: a principal components analysis of the 24-item brief psychiatric rating scale. Psychiatry Res. 97 (2–3), 129–135. [PubMed: 11166085]

Von Holst E, Mittelstaedt H, 1950 Das reafferenzprinzip. Naturwissenschaften 37, 464–476.

Wechsler D, 2011 Wechsler Abbreviated Scale of Intelligence–Second Edition (WASI-II). NCS Pearson, San Antonio, TX.

Whitfield-Gabrieli S, Thermenos HW, Milanovic S, Tsuang MT, Faraone SV, McCarley RW, Shenton ME, Green AI, Nieto-Castanon A, LaViolette P, Wojcik J, Gabrieli JD, Seidman LJ, 2009 Hyperactivity and hyperconnectivity of the default network in schizophrenia and in first-degree relatives of persons with schizophrenia. Proc. Natl. Acad. Sci. U. S. A 106 (4), 1279–1284. [PubMed: 19164577]

Woodward ND, Rogers B, Heckers S, 2011 Functional resting-state networks are differentially affected in schizophrenia. Schizophr. Res. 130 (1–3), 86–93. [PubMed: 21458238]

Yan CG, Wang XD, Zuo XN, Zang YF, 2016 DPABI: data processing & analysis for (resting-state) brain imaging. Neuroinformatics 14 (3), 339–351. [PubMed: 27075850]

Yu Q, Allen EA, Sui J, Arbabshirani MR, Pearlson G, Calhoun VD, 2012 Brain connectivity networks in schizophrenia underlying resting state functional magnetic resonance imaging. Curr. Top. Med. Chem 12 (21), 2415–2425. [PubMed: 23279180]

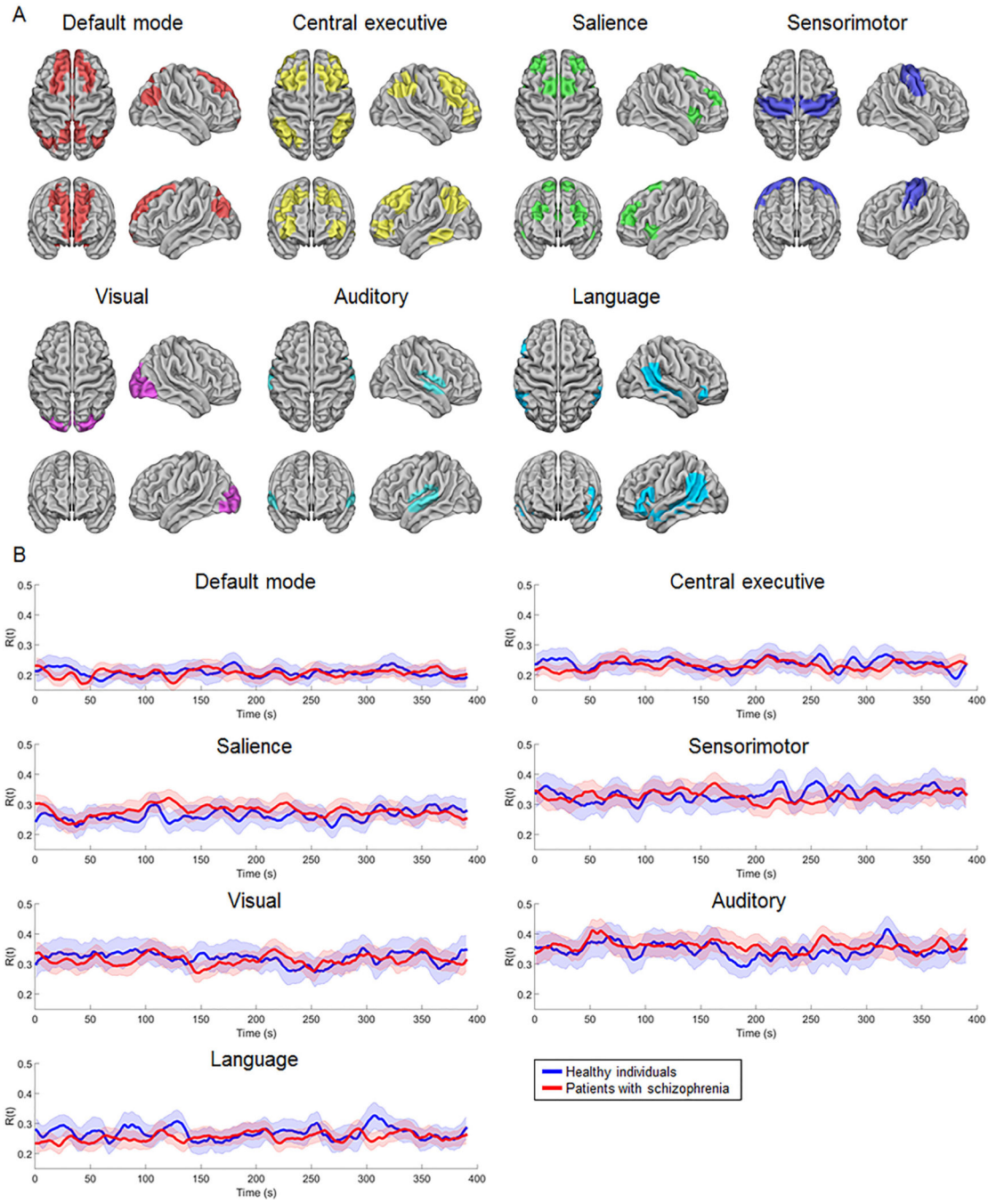

Fig. 1. Temporal synchronization in resting-state networks.

(A) Spatial maps of the 7 resting-state networks, (B) Temporal fluctuations of the order parameter amplitude R(t) of the functional magnetic resonance imaging (fMRI) signal for each RSN. Color-coded thick lines and shaded bands indicate, respectively, the mean and standard error of mean (SEM) of the order parameter amplitudes across subjects for healthy individuals (blue) and patients with schizophrenia (red). Network synchrony and metastability were computed as the mean and standard deviation of the order parameter R(t) over time, respectively.

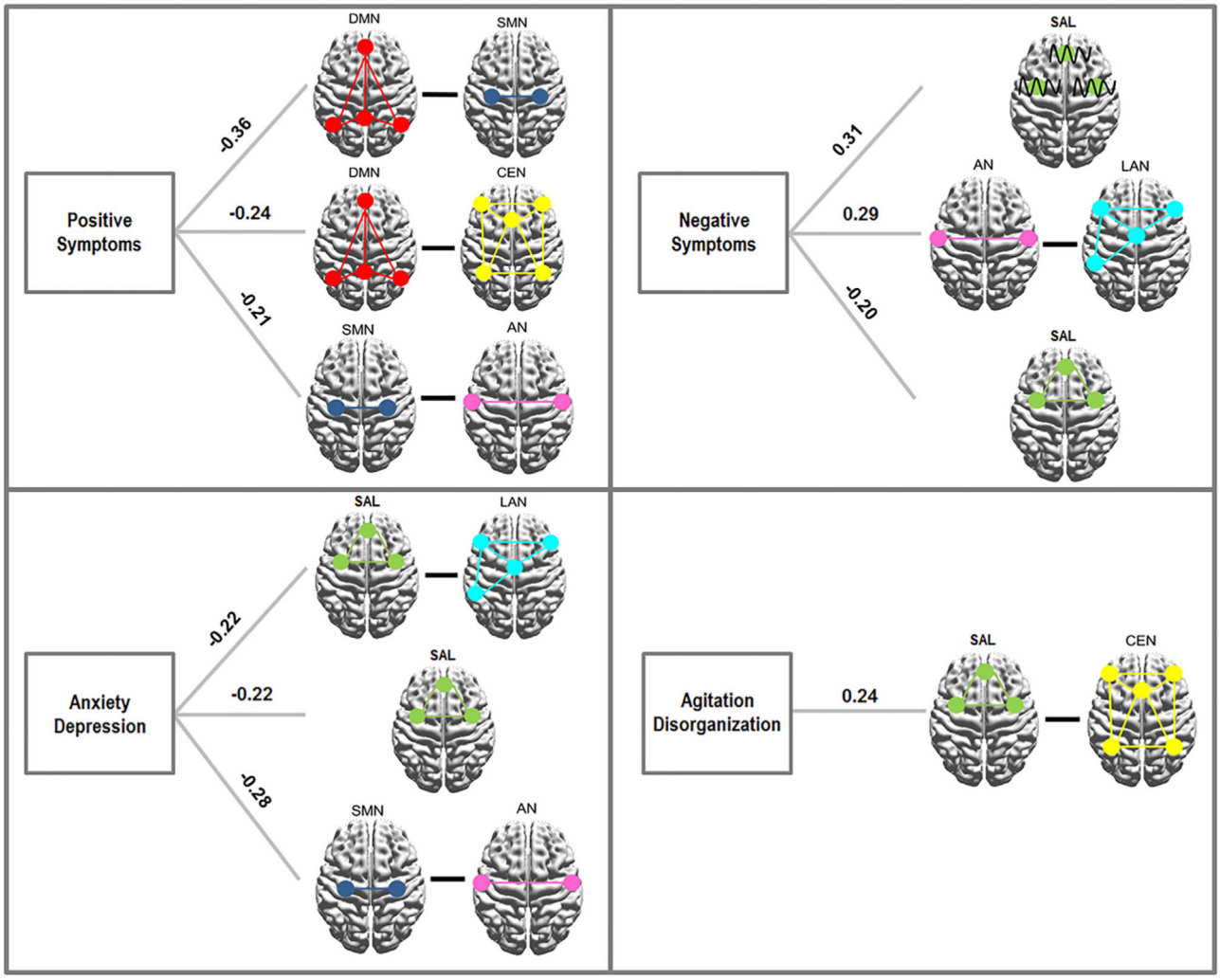

Fig. 2. Schematic presentation of the results of regression analyses.

(A) Positive symptoms, (B) Negative symptoms, (C) Anxiety/Depression, (D) Agitation/ Disorganization. Each network is presented as a simplified diagram of its key nodes for ease of visualization. Lines connecting the nodes of each network represent its within-network functional connectivity. Lines connecting two networks represent their between-network functional connectivity. Signal representation over the key nodes of a network represents the network's metastability. For each significant model for each symptom cluster the standardized coefficients of the significant predictor variables (β). The details of the regression analyses are shown in Table 2. AN: auditory network, CEN: central executive network, DMN: default mode network, LAN: language network, SAL: salience network, SMN: sensorimotor network.

Table 1

Sample Characteristics.

	Patients with schizophrenia (*N* = 85)	Healthy individuals (*N* = 48)
Age (years)	27.18 (7.31)	29.35 (8.28)
Sex (male: female)[1]	64:21	28:20
IQ[2]	93.85 (14.87)	115.87 (16.32)
Duration of illness (years)	5.72 (6.14)	n/a
BPRS positive symptoms[1*]	12.57 ± 6.17	4 (0)
BPRS negative symptoms[1*]	6.83 ± 3.68	3.02 (0.14)
BPRS anxiety/depression[1*]	9.06 ± 5.35	4.02 (0.14)
BPRS agitation/disorganization[1*]	9.57 ± 5.81	6.02 (0.14)
Any medication, n (%)	79 (92.94)	n/a
Antipsychotics, n (%)	75 (88.23)	n/a
Antipsychotic dose (CPZE)	277.24 (246.99)	n/a
Antidepressants, n (%)	23 (27.06)	n/a

Continuous variables are shown as mean (standard deviation); Categorical variables are shown as number of cases (n) and percentage (%); BPRS=Brief Psychiatric Raring Scale

[*] In BPRS symptoms are coded as 1 (absent) to 7 (extremely severe); BPRS positive symptoms = sum of the scores for hallucination, unusual thought content, bizarre behavior subscales; BPRS negative symptoms = sum of the scores for blunted affect, emotional withdrawal, motor retardation subscales; BPRS Depression/Anxiety Scores = sum of the scores for anxiety, depression, suicidality, guilt subscales; BPRS Agitation/Disorganization Scores = sum of scores for motor hyperactivity, elevated mood, excitement, distractibility, grandiosity subscales. CPZE = chlorpromazine equivalents; n/a = not applicable

[1] $p = 0.01$

[2] $p < 0.001$.

Table 2

Summary of Stepwise Regression Analyses for Neuroimaging Predictors of Symptom Severity in Patients with Schizophrenia.

	Positive symptoms					
model	**Variable**	**B (SE B)**	**β**	**Adjusted R^2**	**F**	***P*-value**
1	DMN-SMN	−7.30 (3.33)	−0.23	0.04	4.80	0.03
2	DMN-SMN	−10.38 (3.47)	−0.33	0.10	5.54	0.006
	DMN-CEN	−6.79 (2.77)	−0.27			
3	DMN-SMN	−11.29 (3.43)	−0.36	0.14	5.27	0.002
	DMN-CEN	−6.06 (2.74)	−0.24			
	SMN-AN	−7.02 (3.40)	−0.21			
	Negative symptoms					
1	SAL-meta	49.26 (18.88)	0.27	0.07	6.80	0.01
2	SAL-meta	54.46 (18.23)	0.30	0.14	7.61	0.001
	AN-LAN	4.70 (1.68)	0.28			
3	SAL-meta	55.84 (17.88)	0.31	0.17	6.72	0.0004
	AN-LAN	4.83 (1.64)	0.29			
	SAL	−23.24 (11.17)	−0.20			
	Anxiety/depression					
1	SMN-AN	−6.92 (3.01)	−0.24	0.05	5.29	0.02
2	SMN-AN	−7.73 (2.98)	−0.27	0.08	4.74	0.01
	SAL	−34.65 (17.31)	−0.21			
3	SMN-AN	−8.00 (2.92)	−0.28	0.12	4.76	0.004
	SAL	−36.42 (16.98)	−0.22			
	SAL-LAN	−6.06 (2.89)	−0.22			
	Agitation/disorganization					
1	SAL-CEN	6.18 (2.71)	0.24	0.05	5.20	0.02

AN = auditory network; DMN = default mode network; CEN = central executive network; LAN = language network; SAL = salience network; SMN = somatosensory network; Meta = abbreviation for metastability; when the name of a network is used alone it denotes the within-network functional connectivity of that particular network; between-network connectivity is denoted by joining the names of the respective networks with a hyphen.

B: unstandardized B coefficient, SE B: standard-error of the B coefficient.